

Empirical algorithms for Secchi disk depth using optical and microwave remote sensing data from the Gulf of Finland and the Archipelago Sea

Yuanzhi Zhang, Jouni Pulliainen, Sampsa Koponen and Martti Hallikainen

Laboratory of Space Technology, Helsinki University of Technology, P.O. Box 3000, FIN-02015 HUT, Finland

Zhang, Y., Pulliainen, J., Koponen, S. & Hallikainen, M. 2003: Empirical algorithms for Secchi disk depth using optical and microwave remote sensing data from the Gulf of Finland and the Archipelago Sea. *Boreal Env. Res.* 8: 251–261. ISSN 1239-6095

In this paper empirical algorithms for determining the Secchi disk depth (SDD) are developed and employed using optical (e.g., Landsat TM) and microwave (e.g., ERS-2 SAR) remote sensing data from the Gulf of Finland and the Archipelago Sea. The SDD is an important optical measure of water quality in the study area, where the coastal water considerably attenuates light because of the presence of phytoplankton, suspended matter and yellow substance. The results show that the accuracy of SDD estimation using a neural network-based method is much higher than that of a semi-empirical or multivariate approach. On the other hand, the additional use of SAR data only slightly improved SDD estimation when compared with the use of TM data only. Although the improvement is marginal, the results suggest that there may be some SAR backscattering signatures correlated to SDD measurements in the area. However, such a small improvement is not very helpful for the practical estimation of SDD. In the future, the technique of using combined optical and microwave data still needs to be refined using, e.g., MERIS and ASAR data.

Introduction

Up to the present, the digital evaluation of satellite sensors' information at visible and near infrared (NIR) wavelengths has been used to estimate water quality variables (*see e.g. Klemas et al. 1974, Alföldi and Munday 1978, Moore 1980,*

Shih and Gervin 1980, Carpenter and Carpenter 1983, Verdin 1985, Ferrari et al. 1996). These investigations suggest that Landsat TM can provide relatively low-cost, simultaneous information on surface water conditions from numerous lakes and coastal areas situated within a large geographic area (Lathrop and Lillesand 1986,

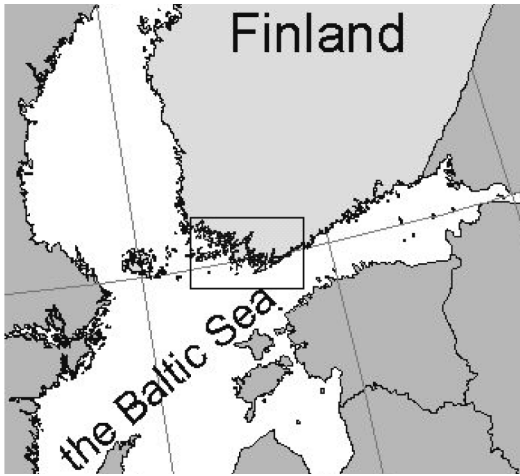


Fig. 1. A map of the study area.

Tassan 1987, Doerffer *et al.* 1989, Harrington and Schiebe 1992, Lindell *et al.* 1999).

The Gulf of Finland and the Finnish Archipelago Sea are optically dominated by scattering from suspended matter, whereas the coastal waters are dominated by absorption from phytoplankton, suspended sediment and yellow substance. This is because the Gulf of Finland and the Archipelago Sea are highly affected by the input from rivers, which discharge a high concentration of suspended mineral solids and nutrients. The optical properties of the water in the area have been studied using remotely sensed data from both space satellites and aircraft (Eloheimo *et al.* 1998, Hallikainen 1999, Harma *et al.* 2001, Koponen *et al.* 2001, Pulliainen *et al.* 2001, Koponen *et al.* 2002, Herlevi 2002).

The Secchi disk depth (SDD) is an important optical characteristic of water related to water quality. It differs, for example, from the suspended sediment concentration which is a measure of the weight of organic and inorganic particulates suspended in the water column (Harrington and Schiebe 1992, Schiebe *et al.* 1992). SDD has already become a widely used tool for measuring water transparency with remote sensing methods (Lathrop and Lillesand 1991, Mausel *et al.* 1991, Dekker and Peters 1993, Lavery *et al.* 1993, Mulhearn 1995). Although there have been many efforts to map this variable from satellite imagery, e.g., from Landsat TM data, the results from deriving water qual-

ity variables from individual scenes are not very consistent (Lindell *et al.* 1999). Fortunately, some advanced optical sensors such as SeaWiFS, MODIS and MERIS are able to provide a better understanding of water quality characteristics, since they can measure the radiance leaving the surface water in six or more bands at visible and near infrared (NIR) wavelengths (Ruddick *et al.* 2000).

Microwave remote sensing, on the other hand, is significantly related to the surface roughness of water. That is, the SAR sensor measures water surface properties rather than those of the water mass below the surface. Since all the features in SAR imagery of water areas are necessarily surface phenomena, all structures in SAR images are related to the surface roughness. On the other hand, surface roughness affects optical interpretations of water quality observations (Lindell *et al.* 1999, Zhang *et al.* 2002a); it may therefore be useful to employ SAR data to assist in the retrieval of water quality variables.

In this study, we first employ a semi-empirical SDD algorithm using the green band of Landsat TM (denoted by TM2). Secondly, tests are made of multivariate regression and neural network algorithms for determining SDD, applying various different TM bands and SAR data for the Gulf of Finland and the Archipelago Sea. The time period is August 1997. In this study, the results of using various empirical algorithms are also compared with each other.

Study area and *in situ* data

The Gulf of Finland is strongly eutrophic because of the anthropogenic nutrient load (e.g., Tamminen 1990, Astok *et al.* 1991, Pitkänen *et al.* 1993, Kuusisto *et al.* 1998). The Gulf is relatively shallow, with a mean depth of 38 m and a maximum depth of 123 m. The total water volume is about 1130 km³. The surface area (29 600 km²) is small as compared with the catchment area (421 000 km²). The incoming river discharge is about 110 km³/year. In the easternmost part of the Gulf the salinity is very low because of the fresh water outflow of the Neva river. The average salinity on the surface is close to 0.6‰ in December and 0.3‰–0.6‰ in June.

The Gulf is also saline-stratified, and in summer temperature-stratified. In general, the concentration of phytoplankton is nitrogen-limited, but in the inner Neva estuary it is phosphorus-limited. The factors affecting light attenuation (organic, inorganic matter and yellow substance) vary temporally as well as spatially (Kuusisto *et al.* 1998). The Archipelago Sea is adjacent to the western part of the Gulf. The study area covers the coastal waters of both regions. Figure 1 shows a map of the study area.

In this case study, concurrent *in situ* measurements of water transparency (i.e., SDD) were collected, and one scene each of both Landsat TM and ERS-2 SAR covering the Gulf of Finland and the Archipelago Sea were obtained. The acquisition times of the TM image and the SAR image were 8.44 UTC and 9.40 UTC on 16 August 1997, respectively. *In situ* measurements (including chlorophyll *a*, suspended sediment and yellow substance) using ship-borne equipment were conducted by the Finnish Environment Institute from 10:00 to 17:50 on 14 August 1997.

Landsat TM and ERS-2 SAR data

A comparison of nearly simultaneous spaceborne optical and microwave observations was possible for the satellite image pair employed in the study. On 16 August 1997, the Landsat TM sensor and the ERS-2 SAR imaged the same coastal region at 8.44 UTC and 9.40 UTC, respectively. Since the time difference between the imaging was less than an hour, the water surface wave conditions, including wind and water temperature, can be assumed to be quite similar for both images (systematic spatial differences in wave conditions). In the previous 24 hours, the average wind speed was about 5.5 m s^{-1} , with a minimum of 3 m s^{-1} and a maximum of 9 m s^{-1} . The wind direction varied from 315 to 360 degrees. The average temperature was $19.5 \text{ }^{\circ}\text{C}$ degrees and the average wave height was about 0.39 m, with a minimum of 0.2 m and a maximum of 0.8 m. Since *in situ* measurements were made on 14 August 1997 and the satellite data were only available on 16 August 1997, we assumed that the water quality conditions were representative for the 16

August 1997, even though the time difference was 2 days (Zhang *et al.* 2002b).

Landsat TM data processing

When satellite data, transformed into radiances as seen by the sensors, are used to retrieve quantitative data concerning the Earth's surface, a procedure to correct the measured radiance for the atmospheric contribution is typically required (Ouaidrari and Vermote 1999, Zhang *et al.* 1999). The remaining amount of radiance that reaches the sensor (target radiance) can range from 25% at 450 nm (the blue region of the electromagnetic spectrum) to 0% at 850 nm (the red region) (Gordon and Morel 1983, Vermote *et al.* 1997, Hu *et al.* 2001, Wang and Gordon 2002).

One technique over water areas is to observe a reflectance target, such as deep clear water, as a "dark object" (Chavez 1988), later improved by the same author (Chavez 1996), that should almost completely absorb all light in the NIR region, and thus should have brightness values close to zero (Gilbert *et al.* 1994). Since analysis was made for a single image with quite a small angular range, the atmospheric correction has little effect on the correlation analysis. Therefore, the atmospheric correction was ignored in this case study.

ERS-2 SAR combined with Landsat TM

Radar remote sensing is quite different from optical remote sensing in many ways. A spaceborne radar is an active instrument that transmits a coherent signal into the target and measures the backscattered signal. Since the wavelengths employed by microwave radars are on the cm scale instead of the nm scale, the interaction of the electromagnetic radiation with a water body is also different from the optical/IR case. A microwave radar signal does not significantly penetrate into the water. Instead it reflects from the water surface. Hence, the radar backscattering signatures can only carry information on (a) water surface geometry (waves and ripples), (b) material on the water surface and (c) the permittivity (dielectric constant) of the top layer of the

water. Nevertheless, water surface geometry can be related to such properties as water depth, internal waves/currents and slicks on the surface (Lindell *et al.* 1999).

One basic assumption in the investigations conducted has been that, since SAR observations are only affected by the surface and since the interpretation of optical data is disturbed by surface reflection, it may be possible, using concurrent SAR data, to correct factors disturbing optical signatures. In practice, the feasibility of this assumption was tested in this study by examining the correlation between the observed TM-intensities and the ERS-2 SAR derived backscattering coefficients.

In order to eliminate the effect of incidence/reflection angle variation within the TM and SAR images, the spatial range in the investigations was limited to 60 km (across-track range for both images). Moreover, an angular correction was made for SAR signatures (normalization to an incidence angle of 19.5°). This was done due to the strong dependence of water surface backscattering on the angle of incidence, which is evident for ERS-2 SAR data even for as small a spatial range as 60 km. The correction was performed by applying an exponential model presented by Ulaby *et al.* (1982).

Empirical algorithms

Typically, many retrieval algorithms in the literature are based on some logarithmic relation of the reciprocal of SDD (Lindell *et al.* 1999). In this study, we employed and compared the results from different kinds of algorithms: (a) a semi-empirical algorithm for SDD using channel 2 (TM2) of Landsat TM, (b) multivariate regression and (c) neural network methods for SDD using optical (TM) data and microwave (SAR) data in the study area.

A semi-empirical algorithm

The Secchi disk depth (m), SDD, for monochromatic light is written (Hojerslev 1986) as

$$\text{SDD} = 6.3/c \quad (1)$$

where c is the attenuation coefficient (m^{-1}). However, for turbid waters, the contribution to the light attenuation mainly comes from scattering, and thus c is independent of wavelength (Phillips and Kirk 1984). This means that Eq. 1 can be considered as a good approximation for the naked eye, without filters (Mulhearn 1995).

Absorption, backscattering and attenuation coefficients (a , b_B and c , respectively) can be further expressed as follows (e.g., Bukata *et al.* 1995)

$$a = a_w + a_{ch} + a_{sm} + a_{ys}, \quad (2a)$$

$$b_B = 0.5b_w + b_{B, ch} + b_{B, sm}, \quad (2b)$$

$$c = c_w + c_{ch} + c_{sm} + c_{ys}, \quad (2c)$$

where the subscripts w, ch, sm, ys and B refer to the contributions from pure sea water, phytoplankton, suspended sediment, yellow substance and backscattering, respectively. Also, $0.5b_w = b_{B, w}$, where b_w is the scattering coefficient for pure sea water (Jerlov 1976).

The coastal waters of the Gulf of Finland and the Archipelago Sea are predominantly green to blue-green, except in the plumes of rivers after heavy rain. This means that a submerged Secchi disk can be viewed in a wavelength band similar to that of Landsat TM band 2, i.e., 520–600 nm. Thus, for this band it is reasonable to assume that the effects of yellow substance are negligible (Jerlov 1976). In this band there is a minimum in absorption by phytoplankton (Shifrin 1988). Let us therefore assume that both phytoplankton and suspended sediment are purely scattering centres. That is, their absorption can be also ignored in this band, i.e., both a_{ch} and a_{sm} are considerably smaller than a_w . Then we can obtain as follows

$$a = a_w, \quad (3a)$$

$$b_B = 0.5b_w + b_{B, ch} + b_{B, sm}, \quad (3b)$$

$$c = c_w + c_{ch} + c_{sm}. \quad (3c)$$

The remote sensing reflectivity, R , is given (Gordon and Morel 1983) by

$$R = 0.33b_B/a, \quad (4)$$

where R is the ratio of upwelling to downwelling irradiance just below the sea surface, b_B is the backscatter coefficient, and a is the absorption coefficient.

Now, Eq. 4 can be written as

$$R = 0.33(0.5b_w + b_{B_{ch}} + b_{B_{sm}})/a_w \quad (5)$$

where R is the reflectivity in the green band (TM2).

According to Mulhearn (1995) and Bukata *et al.* (1995), let us define the relation between total scatter and backscatter by setting $b_{B_{ch}} + b_{B_{sm}} = Bb_{ch} + Bb_{sm} = Bc_{ch} + Bc_{sm} = B(c_{ch} + c_{sm})$, where B is the ratio of backscatter to the total scattering coefficient for both phytoplankton and suspended sediment and is assumed to be the same for both of them. Therefore, Eq. 5 can also be expressed as

$$R = 0.33(B(c_{ch} + c_{sm}) + 0.5b_w)/a_w. \quad (6)$$

From Eqs. 1 and 3c ($c = c_w + c_{ch} + c_{sm}$), we can obtain

$$c_{ch} + c_{sm} = 6.3/SDD - c_w, \quad (7)$$

and then

$$R = 0.33(B(6.3/SDD - c_w) + 0.5b_w)/a_w, \quad (8)$$

where B is the only adjustable constant in this equation. Values quoted in the literature for the ratio of backscatter to the total scattering coefficient for ocean waters, not just for both phytoplankton and suspended matter, i.e., for all particles, range between 0.006 and 0.11 (Mankovskiy 1984, Shifrin 1988). The theoretical value for pure water is 0.5. Values for coastal waters appear to range between 0.006 and 0.025 (Mulhearn 1995). The assumptions in Eq. 8 imply that both c_{ch} and c_{sm} are much greater than c_w and that $6.3B/SDD$ is also much greater than $0.5b_w$. Given a value for B of approximately 0.01 and taking $c_w = 0.066 \text{ m}^{-1}$ and $b_w = 0.002 \text{ m}^{-1}$ (Hojerslev 1986) for 520–600 nm, both of these assumptions will be satisfied if $SDD \ll 100 \text{ m}$, which is always true in coastal waters.

Thus, Eq. 8 can be written as

$$R = 0.33(6.3B/SDD)/a_w \quad (9)$$

and with $a_w = 0.064 \text{ m}^{-1}$ (Hojerslev 1986),

$$SDD = 32.5B/R \quad (10)$$

as also obtained by Mulhearn (1995). The semi-empirical algorithm given by Eqs. 9 and 10 assumes that absorption both by yellow substance and by phytoplankton were negligible in the study material. This may cause inaccuracy in SDD retrieval. Further studies are still needed to refine this semi-empirical algorithm.

Multivariate algorithms

A radar measurement is affected by target properties different from those for optical/IR observations. At optical wavelengths, however, the passive remote sensing observations are affected by the volume scattering and fluorescence of incoming solar radiation inside the water body. The temporal and spatial variations in water surface roughness are actually factors that disturb the interpretation of optical data. Since the radar observations are only influenced by the surface layers, it may be possible to develop water quality retrievals in which SAR data are used to provide supplementary information for optical observations (Lindell *et al.* 1999, Zhang *et al.* 2002a).

In this case study, the SDD multivariate algorithms derived from TM bands and from combined TM/SAR data can be expressed as follows

$$SDD_{TM} = A_0 + \sum_{i=1}^7 A_i(TM_i) \quad (11)$$

$$SDD_{TM/SAR} = B_0 + \sum_{i=1}^7 B_i(TM_i) + B(SAR) \quad (12)$$

where TM_i and SAR can be the digital number (DN) values of the 7 TM bands and SAR data while A_0 , A_i , B_0 , B_i , and B are the derived regression coefficient values, which can be obtained by comparing the satellite observations with the measurements from ground truth points.

An empirical neural network algorithm

An empirical neural network algorithm was also applied in this case study. A neural network has three layers: input layer, hidden layer, and output layer. The first (input) layer distributes the input parameters, i.e., the data extracted at

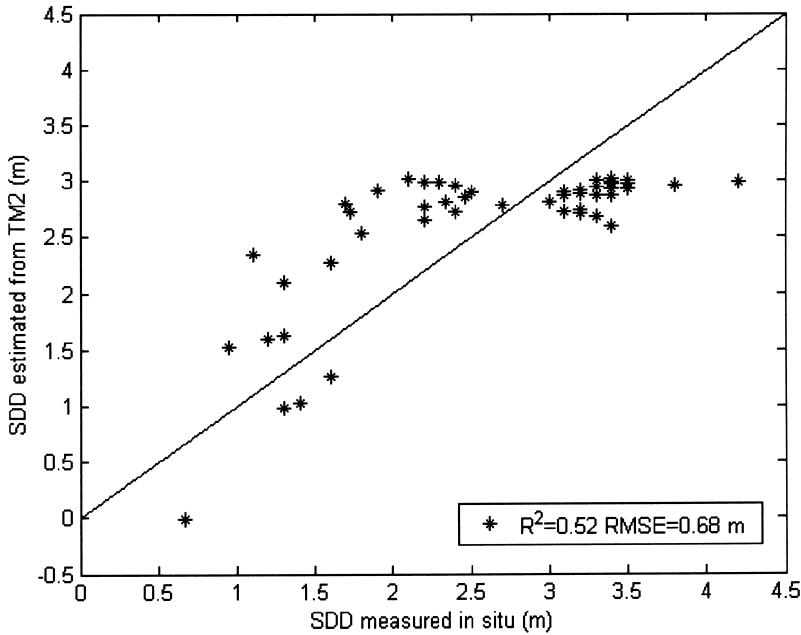


Fig. 2. Regression of SDD estimated from TM2 with the measured SDD using the semi-empirical algorithm.

different wavelengths (TM and SAR observations), to the second layer. The second (hidden) layer has a varying number of neurons, where each input parameter is multiplied by its connection's weights and all the inputs to the neurons are summed and passed through the non-linear sigmoid function. The third layer receives the output of the second layer and processes this through neurons again (Keiner and Yan 1998, Keiner 1999).

In a neural network, each neuron has two parts: a linear summation function and a non-linear activation function. The inputs to each neuron are firstly routed through the summation function. The output of this function inside the neuron at node j is given by

$$y_j = \sum_{i=1}^n w_{ij}x_i + b_j \quad (13)$$

where x_i are the inputs, w_{ij} are the weights related to each input/node connection, and b_j is the bias related to node j , and y_j is the output of this function inside the neuron at node j .

The inputs to the neuron are multiplied by their related weights, summed and added to the bias. The weights determine which inputs and connections in the network are more important

than others. The bias controls the activation level of a neuron, when the resulting sum is passed through a non-linear activation function

$$\begin{aligned} \text{SDD} &= g(y_j) = a \tanh(y_j) \\ &= a \tanh\left(\sum_{i=1}^n w_{ij}x_i + b_j\right) \end{aligned} \quad (14)$$

where g is a sigmoid activation function and a is a factor depending on the valid range of SDD, i.e., the maximum plus one. The activation function is what gives the network its ability to model non-linear behaviour (Krasnopolsky *et al.* 1995, 2000, Zhang *et al.* 2002c).

Validation against *in situ* data

The potential of satellite remote sensing is to yield synoptic information on water transparency over large areas. However, the limitation of this technology includes the fact that the accuracy of water quality information is related to the accuracy and representativeness of *in situ* water sampling (Eloheimo *et al.* 1998, Hallikainen 1999). In this case study, the validation of SDD retrieval against *in situ* data ranges from 0.67 to 4.2 meters.

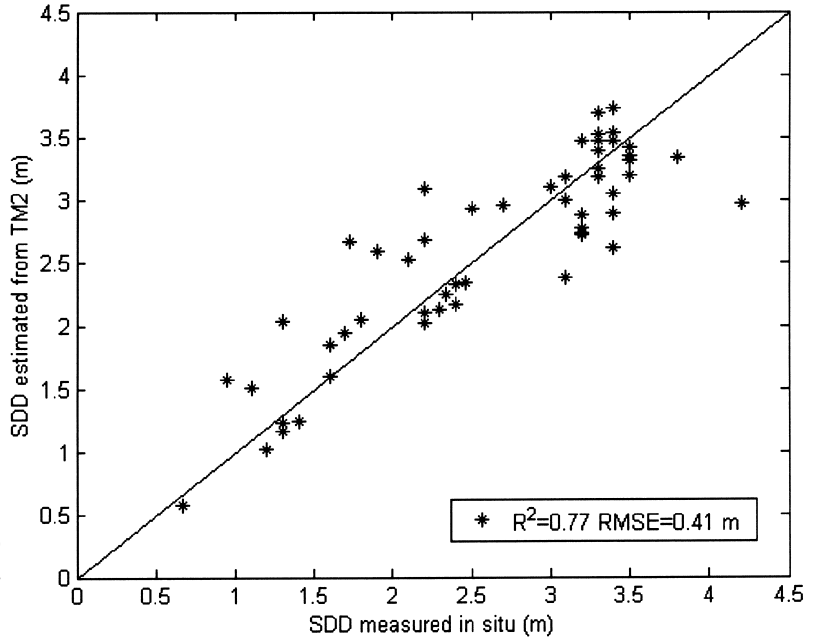


Fig. 3. Regression of SDD estimated from TM/SAR data with the measured SDD using the multivariate approach.

Results and discussion

With Eq. 10, SDD derived from TM2 is plotted against the measured SDD in Fig. 2. For this algorithm, the coefficient of determination is $R^2 = 0.52$, the root mean square error is $RMSE = 0.68$ m, and the adjustable constant $B = 0.0167$. Clearly, this result is not good enough for practical SDD retrieval in the coastal waters of the study area. The main reason for this is probably that we assumed the absorption by yellow substance and by phytoplankton to be negligible in the semi-empirical algorithm.

Using the digital number values of the TM bands and SAR data, SDD can also be directly estimated with the multivariate algorithms (Eqs. 11 and 12, respectively). Thus, SDD can be obtained from

$$\begin{aligned} SDD_{TM} = & 1.878 + 0.043(TM1) + \\ & 0.002(TM2) - 0.142(TM3) - \\ & 0.256(TM4) + 0.018(TM5) + \\ & 0.008(TM6) + 0.005(TM7) \end{aligned} \quad (15)$$

with the coefficient of determination $R^2 = 0.74$ and $RMSE = 0.44$ m.

$$\begin{aligned} SDD_{TM/SAR} = & 3.452 + 0.029(TM1) - \\ & 0.009(TM2) - 0.079(TM3) - 0.375(TM4) + \\ & 0.127(TM5) + 0.007(TM6) - \\ & 0.010(TM7) - 0.003(SAR) \end{aligned} \quad (16)$$

with the coefficient of determination $R^2 = 0.77$ and $RMSE = 0.41$ m (Fig. 3).

Obviously, the multivariate regression approach was better at retrieving SDD than the semi-empirical algorithm ($R^2 = 0.52$). However, SAR data only improved SDD estimation slightly in this case study. However, this small SDD improvement (3%) may suggest that there are some backscattering signatures of the SAR data observation corresponding to surface properties in SDD measurements in the area.

On the other hand, the results indicated that the accuracy of SDD estimation applying the neural network ($R^2 = 0.95$ and $RMSE = 0.19$ m for TM/SAR (Fig. 4) and $R^2 = 0.91$ and $RMSE = 0.25$ m for TM only) is much greater than that of the semi-empirical algorithm ($R^2 = 0.52$) or multivariate approach ($R^2 = 0.77$ for TM/SAR and $R^2 = 0.74$ for TM) (see Table 2). SAR data improved SDD estimation in the study by less than 5% (e.g., 4% for the neural network method). Further studies are needed using simul-

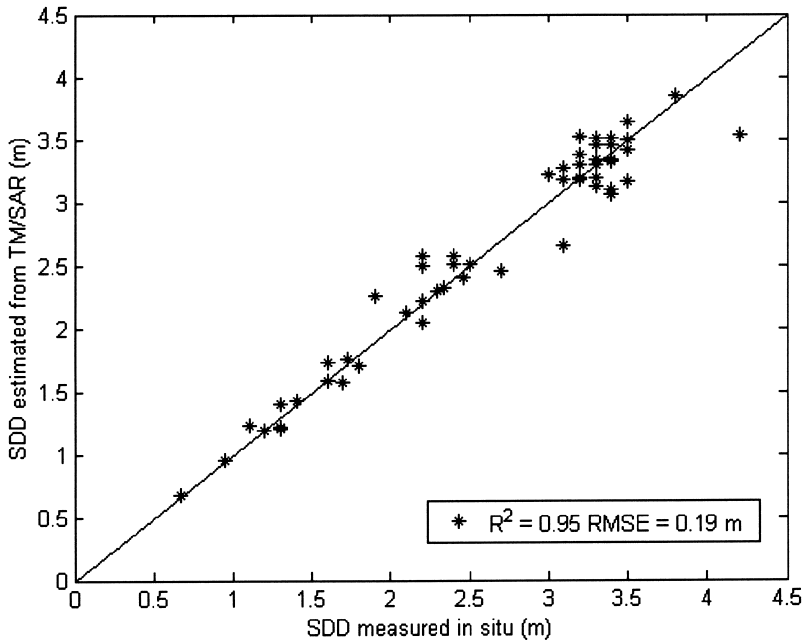


Fig. 4. Regression of SDD estimated TM/SAR data with the measured SDD using the neural network algorithm.

taneous acquisition of optical and SAR data, e.g., MERIS and ASAR, in the area.

An examination of the correlations between the digital values of the different TM bands showed that the correlations (r^2) for TM band 1–7 pairs ranged between 0.00 and 0.93. This difference among the bands may imply that the blue band (TM1), green band (TM2), red band (TM3), and near infrared band (TM4), as well as TM5, TM6 and TM7 either changed greatly at any one site or changed differently at all sites. This may also have a significant effect on the results of data analysis in this study (Zhang *et al.* 2002b). Moreover, the high correlation between some TM bands means that these are measuring similar optical properties of the water in the study area.

Examination also indicated that SDD had a correlation (r^2) of 0.31 with chlorophyll *a* and a correlation (r^2) of 0.49 with suspended sediment

concentration. That is, SDD has some correlations with amounts of both organic and inorganic matter in the study area (Zhang *et al.* 2002b).

Table 1 gives the correlation (r^2) between SDD and the digital data of the TM bands and ERS-2 SAR. Simple regression analysis indicated that SDD has its highest correlation with TM3 ($r^2 = 0.53$), and higher correlations with TM2 and TM4 than with TM1, but a low correlation with TM5 and very low correlations with TM6 and TM7. However, ERS-2 SAR has some correlation with the variation of SDD ($r^2 = 0.36$).

A previous study (Zhang *et al.* 2002a) showed that the highest correlation between TM and SAR data was that between TM2 and SAR data ($r^2 = 0.14$). Since angular corrected SAR observations are only dependent on the surface wave conditions (in addition to random speckle, which was mostly averaged out in the employed

Table 1. Correlation (r^2) between Secchi disk depth (SDD) and the digital data of TM bands and ERS-2 SAR.

	TM (450– 520 nm)	TM2 (520– 600 nm)	TM3 (630– 690 nm)	TM4 (760– 900 nm)	TM5 (1550– 1750 nm)	TM6 (2080– 2350 nm)	TM7 (10400– 12500 nm)	SAR (C-band)
SDD	0.20	0.38	0.53	0.46	0.16	0.06	0.07	0.36

water area signatures), this suggests that the variations in wave conditions in different parts of the TM image caused 14% of the variability in the TM2 observations.

Table 2 gives a comparison of SDD estimation results using the empirical algorithms for TM data and SAR data. The results show that SDD retrieval values obtained using the semi-empirical algorithm are lower than those expected for coastal waters in the area. Probably, this is because we assumed the absorption by yellow substance and by phytoplankton to be negligible in the study. Obviously, the semi-empirical algorithm needs to be refined in future studies. Even though the multivariate regression approach using TM data improved SDD ($R^2 = 0.74$) estimation over that obtained using the semi-empirical algorithm ($R^2 = 0.52$), the additional use of SAR data did not improve the SDD estimation much ($R^2 = 0.77$). Similarly, the accuracy of the SDD estimation applying the neural network ($R^2 = 0.91$) to TM data is much greater than that of those from the semi-empirical algorithm and multivariate approach. However, SAR data did improve SDD retrieval slightly.

In the international literature, the mapping of SDD has shown similar results. The results for individual scenes are not very consistent and show variability in R^2 from 0.59 to 0.98 (Lindell *et al.* 1999). For example, Dekker and Peters (1993) found the following relations

$$\text{SDD} = 1199.93 - 55.90(\text{TM3}) \quad (17)$$

where TM3 is a digital number and $R^2 = 0.66$.

$$\ln(\text{SDD}) = 37.36 - 11.15\ln(\text{TM3}) \quad (18)$$

with $R^2 = 0.86$.

Ghezzi *et al.* (1998) reported a relationship with $R^2 = 0.749$ for SDD ranging from 8.0 to 9.5 m using

$$\text{SDD} = 10.41 - 46.54\ln(R_{\text{TM2}}). \quad (19)$$

Lathrop *et al.* (1991) used reflectance values derived from TM1 and TM3 and obtained $R^2 = 0.87$ with the following function

$$\text{SDD} = 208e^{-9.82\frac{R_{\text{TM3}}}{R_{\text{TM1}}}}. \quad (20)$$

Lavery *et al.* (1993) got $R^2 = 0.81$ for the relation

$$\text{SDD} = 0.74 - 0.05R_{\text{TM3}} + 1.80\frac{R_{\text{TM1}}}{R_{\text{TM3}}}. \quad (21)$$

Conclusions

In this study empirical algorithms have been developed and applied for obtaining the Secchi disk depth using optical (e.g., Landsat TM) and microwave (e.g., ERS-2 SAR) remote sensing data from the Gulf of Finland and the Archipelago Sea. The digital TM and SAR data from water sample locations were extracted and examined. Significant correlation was observed between the digital data and SDD. The results show that SDD can be estimated in the coastal waters of the study area using a semi-empirical algorithm, multivariate algorithms or neural network algorithms. The results also indicate that the accuracy of the SDD estimation found by applying a neural network ($R^2 = 0.95$ for TM/SAR and 0.91 for TM) is much higher than that of either the semi-empirical algorithm ($R^2 = 0.52$) or the multivariate approach ($R^2 = 0.77$ for TM/SAR and 0.74 for TM). SAR data improved SDD estimation by less than 5%

Table 2. Comparison of Secchi disk depth (SDD) using empirical algorithms derived from TM and from TM/SAR data.

	Semi-empirical algorithm (R^2 & RMSE)	Multivariate regression (R^2 & RMSE)	Neural network (R^2 & RMSE)
TM	0.52 & 0.68 m	0.74 & 0.44 m	0.91 & 0.25 m
TM/SAR	NA	0.77 & 0.41 m	0.95 & 0.19 m

Note: NA means not available for the semi-empirical algorithm.

(e.g., 3% for the multivariate approach and 4% for the neural network method). Although SAR improved SDD retrieval slightly, the results may suggest that there are some SAR backscattering signatures corresponding to SDD measurements in the area. It may also be useful to develop SDD algorithms in which SAR data are used as supplementary data to optical observations of water transparency characteristics. Such small improvements do not appear to be very helpful for practical SDD retrieval in the area.

Acknowledgements: We would like to thank K. Eloheimo, K. Kallio, T. Hannonen, P. Härmä, T. Kutser, T. Pyhälähti, J. Vepsäläinen, Y. Sucksdorff, J. Kämäri, J. Vuorimies, H. Servomaa, S. Taurainen, M. Euro and P. Karlsson for providing necessary support. We would also thank two reviewers for their scientific comments through the manuscript.

References

- Alföldi T. & Munday J. C. 1978. Water quality analysis by digital chromaticity mapping of Landsat data. *Canadian J. Remote Sens.* 4: 108–122.
- Astok V., Hannus M. & Jaanus A. 1991. The state of the coastal waters of the eastern part of the Gulf of Finland in the 1980's: General conclusions. *Baltic Sea Environ. Proceedings* 40: 70–74.
- Bukata R.P., Jerome J.H., Kondratyev K.Y.A. & Pozdnyakov D.V. 1995. *Optical properties and remote sensing of inland coastal waters*, CRC Press Inc. Boca Raton, Florida, 362 pp.
- Carpenter D.S. & Carpenter S.M. 1983. Monitoring inland water quality using Landsat data. *Remote Sens. Environ.* 13: 345–352.
- Chavez P.S.Jr. 1988. An improved dark-object subtraction technique for atmospheric scattering correction of multispectral data. *Remote Sens. Environ.* 24: 459–479.
- Chavez P.S.Jr. 1996. Image-based atmospheric corrections-revised and improved. *Photogramm. Eng. Remote Sens.* 62: 1025–1036.
- Dekker A.G. & Peters S.W.M. 1993. The use of the Thematic Mapper for the analysis of eutrophic lakes: a case study in the Netherlands. *Int. J. Remote Sens.* 14: 799–821.
- Doerffer R., Fischer J., Stossel M. & Brockmann C. 1989. Analysis of Thematic Mapper data for studying the suspended matter distribution in the coastal area of the Germany Bight (North Sea). *Remote Sens. Environ.* 28: 61–73.
- Eloheimo K., Hannonen T., Härmä P., Pyhälähti T., Koponen S., Pulliainen J. & Servomaa H. 1998. Coastal monitoring using satellite, airborne and in situ data in the archipelago of Baltic Sea. *Proceed. 5th Int. Conference Remote Sens. Marine and Coastal Environ., San Diego, USA, 5–7 Oct.* pp. 306–314.
- Ferrari G.M., Hoepffner N. & Mingazzini M. 1996. Optical properties of the water in a deltaic environment: prospective tool to analyse satellite data in turbid waters. *Remote Sens. Environ.* 58: 69–80.
- Gilbert M.A., Conese C. & Maselli F. 1994. An atmospheric correction method for the automatic retrieval of surface reflectances from TM images. *Int. J. Remote Sens.* 15: 2065–2086.
- Ghezzi P., Giardino C., Pepe M. & Zilioli E. 1998. Report on the 2nd Salmon joint meeting, Venice. *CEC Progress Report*, (Milano: CNR-IRRS Telerilevamento), pp. 10–11.
- Gordon H.R. & Morel A.Y. 1983. *Remote assessment of ocean color for interpretation of satellite imagery – a review*. Spring-Verlag, New York. 114 pp.
- Hallikainen M. 1999. Development of sensors and methods for remote sensing of Northern areas by HUT laboratory of space technology. *IEEE Geosci. Remote Sens. Newsletter* 107: 10–11.
- Harma P., Vepsäläinen J., Hannonen T., Pyhälähti T., Kamari J., Kallio K., Eloheimo K. & Koponen S. 2001. Detection of water quality using simulated satellite data and semi-empirical algorithms in Finland. *The Science of the Total Environment* 268: 107–121.
- Harrington J.A.Jr. & Schiebe F.R. 1992. Remote sensing of Lake Chicot, Arkansas: monitoring suspended sediments, turbidity, and secchi depth with Landsat MSS data. *Remote Sens. Environ.* 39: 15–27.
- Herlevi A. 2002. *Inherent and apparent optical properties in relation to water quality in Nordic waters*, Ph.D. thesis, Report Series in Geophysics No. 45. University of Helsinki, Division of Geophysics, Helsinki, 132 pp.
- Hojerslev N.K. 1986. Optical properties of sea water. In: Sunderman J. (ed.), *Oceanography*, Spring-Verlag, London, pp. 383–462.
- Hu C.M., Muller-Karger F.E., Andrefouet S. & Carder K.L. 2001. Atmospheric correction and cross-calibration of Landsat-7/ETM+ imagery over aquatic environment: A multiplatform approach using SeaWiFS/MODIS. *Remote Sens. Environ.* 78: 99–107.
- Jerlov N.G. 1976. *Marine optics*. Elsevier, Amsterdam. 231 pp.
- Keiner L.E. & Yan X. 1998. A neural network model for estimating sea surface chlorophyll and sediments from Thematic Mapper Imagery. *Remote Sens. Environ.* 66: 153–165.
- Keiner L.E. 1999. Neural networks as non-linear function approximation for remote sensing applications. In: Chen C.H. (ed.), *Information processing for remote sensing*, World Scientific Publishing Co., Singapore, pp. 213–223.
- Klemas V., Bartlett D., Philpot W. & Roger R. 1974. Coastal and estuarine studies with ERTS-1 and Skylab. *Remote Sens. Environ.* 3: 153–177.
- Koponen S., Pulliainen J., Servomaa H., Zhang Y., Hallikainen M., Kallio K., Vepsäläinen J., Pyhälähti T. & Hannonen T. 2001. An analysis on the feasibility of multi-source remote sensing observations for chl-a monitoring in Finnish lakes. *The Science of the Total Environment* 268: 95–106.

- Koponen S., Pulliainen J., Kallio K. & Hallikainen M. 2002. Lake water quality classification with airborne hyperspectral spectrometer and simulated MERIS data. *Remote Sens. Environ.* 79: 51–59.
- Krasnopolsky V., Breaker L. & Gemmill W. 1995. A neural network as a nonlinear transfer model for retrieving surface wind speeds from the special sensor microwave imager. *J. Geophys. Res.* 100: 11033–11045.
- Krasnopolsky V., Gemmill W. & Breaker L. 2000. A neural network multi-parameter algorithm for SSM/I ocean retrievals: comparisons and validations. *Remote Sens. Environ.* 73: 133–142.
- Kuusisto M., Koponen J. & Sarkkula J. 1998. Modelled phytoplankton dynamics in the Gulf of Finland. *Environ. Modelling and Software* 13: 461–470.
- Lathrop R.G.Jr. & Lillesand T.M. 1986. Use of Thematic Mapper data to assess water quality in Green Bay and central Lake Michigan. *Photogramm. Eng. Remote Sens.* 52: 671–680.
- Lathrop R.G., Lillesand T.M. & Yandell B.S. 1991. Testing the utility simple multi-date Thematic Mapper calibration algorithms for monitoring turbid inland waters. *Int. J. Remote Sens.* 12: 2045–2063.
- Lavery P., Pattiaratchi C., Wyllie A. & Hick P. 1993. Water quality monitoring in estuarine water using the Landsat Thematic Mapper. *Remote Sens. Environ.* 46: 268–280.
- Lindell T., Pierson D., Premazzi G. & Zilioli E. 1999. *Manual for monitoring European lakes using remote sensing techniques*, Official Publications of the European Communities, Luxembourg, 161 pp.
- Mankovskiy V.I. 1984. Spectral variability of the coefficient of asymmetry of the light scattering function by sea water. *Oceanology* 24: 46–51.
- Mausel P.W., Karakaka M.A., Mao C.Y., Escobar D.E. & Everitt J.H. 1991. Insights into secchi transparency through computer analysis of aerial multispectral video data. *Int. J. Remote Sens.* 12: 2485–2492.
- Moore G.K. 1980. Satellite remote sensing of water quality. *Hydro. Sci.* 25: 407–421.
- Mulhearn P.J. 1995. Landsat reflectivities versus Secchi disc depths. *Int. J. Remote Sens.* 16: 257–268.
- Ouaidrari H. & Vermote E.F. 1999. Operational atmospheric correction of Landsat TM data. *Remote Sens. Environ.* 70: 4–15.
- Phillips D.M. & Kirk J.T.O. 1984. Study of the spectral variation of absorption and scattering in some Australia coastal waters. *Australian J. Marine Freshw. Res.* 34: 635–644.
- Pitkänen H., Tamminen T., Kangas P., Huttula T., Kivi K., Kuosa H., Sarkkula J., Eloheimo K., Kauppila P. & Skakalsky B. 1993. Late summer trophic conditions in the north-east Gulf of Finland and the River Neva estuary, Baltic Sea. *Estuarine Coastal and Shelf Science* 37: 453–474.
- Pulliainen J., Kallio K., Eloheimo K., Koponen S., Servomaa H., Hannonen T., Tauriainen S. & Hallikainen M. 2001. A semi-operational approach to water quality retrieval from remote sensing data. *The Science of the Total Environment* 268: 79–93.
- Ruddick K.G., Ovidio F. & Rijkeboer M. 2000. Atmospheric correction of SeaWiFS imagery for turbid coastal and inland waters. *Appl. Opt.* 39: 897–912.
- Schiebe F.R., Harrington J.A. & Ritchie C.B. 1992. Remote sensing of suspended sediments: the Lake Chicot, Arkansas project. *Int. J. Remote Sens.* 13: 1487–1509.
- Shifrin K.S. 1988. *Physical optics of ocean water*, American Institute of Physics, New York. 285 pp.
- Shih S.F. & Gervin J.C. 1980. Ridge regression techniques applied to Landsat investigation of water quality in lake Okeechobee. *Water Resources Bull.* 16: 790–796.
- Tamminen T. 1990. *Eutrophication and the Baltic Sea: studies on phytoplankton, bacterioplankton and pelagic nutrient cycles*. Ph.D. thesis, Department of Environmental Conservation, University of Helsinki, Helsinki.
- Tassan S. 1987. Evaluation of the potential of the Thematic Mapper for marine application. *Int. J. Remote Sens.* 8: 1455–1478.
- Ulaby F.T., Moore R.K. & Fung A.K. 1982. *Microwave remote sensing: active and passive*, vol. II, Addison-Wesley Publishing Company, Reading Massachusetts, pp. 853–860.
- Verdin J.P. 1985. Monitoring water quality in a large western reservoir with Landsat imagery. *Photogramm. Eng. Remote Sens.* 51: 343–353.
- Vermote E.F., Tanre D., Deuze J.L., Herman M. & Morcrette J.J. 1997. Second simulation of the satellite signal in the solar spectrum, 6S: an overview. *IEEE Trans. Geosci. Remote Sens.* 35: 675–686.
- Wang M. & Gordon H.R. 2002. Calibration of ocean color scanners: how much error is acceptable in the near infrared? *Remote Sens. Environ.* 82: 497–504.
- Zhang M., Carder K., Muller-Karger F.E., Lee Z. & Gold D.B. 1999. Noise reduction and atmospheric correction for coastal applications of Landsat Thematic Mapper. *Remote Sens. Environ.* 70: 167–180.
- Zhang Y., Pulliainen J., Koponen S. & Hallikainen M. 2002a. Applicability of combined microwave and optical data for surface water quality retrievals. *J. Electromagn. Waves Appl.* 16: 249–251.
- Zhang Y., Pulliainen J., Koponen S. & Hallikainen M. 2002b. Water quality retrievals from combined Landsat TM data and ERS-2 SAR data in the Gulf of Finland. *IEEE Trans. Geosci. Remote Sens.* 41: 622–629.
- Zhang Y., Pulliainen J., Koponen S. & Hallikainen M. 2002c. Application of an empirical neural network to surface water quality estimation in the Gulf of Finland using combined optical data and microwave data. *Remote Sens. Environ.* 81: 327–336.